Observation of a sequence of wetting transitions in the binary water +ethylene glycol monobutyl ether mixture

Chih-Kang Wu and Li-Jen Chen[a)]
Department of Chemical Engineering, National Taiwan University, Taipei, Taiwan 10617 Republic of China

(Received 20 May 2005; accepted 29 June 2005; published online 30 August 2005)

A homemade pendant drop/bubble tensiometer was assembled and applied to perform the surface-interfacial tension measurements for the binary water+ethylene glycol monobutyl ether (C_4E_1) mixture over the temperature range from 50 to 128 °C at 10 bar. The symbol C_iE_j is the abbreviation of a nonionic polyoxyethylene alcohol $C_iH_{2i+1}(OCH_2CH_2)_jOH$. The wetting behavior of the C_4E_1-rich phase at the interface separating the gas and the aqueous phases was systematically examined according to the wetting coefficient calculated from the experimental results of surface/interfacial tensions. It was found that the C_4E_1-rich phase exhibits a sequence of wetting transitions, nonwetting→partial wetting→complete wetting, at the gas-water interface in the water+C_4E_1 system along with increasing the temperature, consistent with the conjecture of Kahlweit and Busse [J. Chem. Phys. **91**, 1339 (1989)]. In addition, the relationship of the mutual solubility and the interfacial tension of the interface separating the C_4E_1-rich phase and the aqueous phase is discussed. © *2005 American Institute of Physics*. [DOI: 10.1063/1.2008235]

I. INTRODUCTION

Consider three fluid phases, α, β, and γ, in equilibrium under gravity and the densities of these three phases are in the order $\rho_\gamma > \rho_\beta > \rho_\alpha$. The wetting behavior of the middle β phase can be easily realized by the wetting coefficient defined as $W=(\sigma_{\alpha\beta}-\sigma_{\alpha\gamma})/\sigma_{\beta\gamma}$. The symbol σ_{ij} stands for the interfacial tension of the interface separating i and j phases. Based on the wetting coefficient W, the wetting behavior of a small amount of the β phase at the α-γ interface can then be classified into three types, as illustrated in Fig. 1.

(a) $W=1$, a nonwetting β phase at the α-γ interface, as shown in Fig. 1(a). In this case the Antonow's rule[1] is applied in the form $\sigma_{\alpha\beta}=\sigma_{\alpha\gamma}+\sigma_{\beta\gamma}$.
(b) $1>W>-1$, a partial wetting β phase at the α-γ interface, as shown in Fig. 1(b). The relationship between interfacial tensions is $\sigma_{\alpha\beta}-\sigma_{\beta\gamma}<\sigma_{\alpha\gamma}<\sigma_{\alpha\beta}+\sigma_{\beta\gamma}$, which follows the Neumann's inequality.[2]
(c) $W=-1$, a complete wetting β phase at the α-γ interface, as shown in Fig. 1(c). In this case the tensions obey the Antonow's rule,[1] $\sigma_{\alpha\beta}+\sigma_{\beta\gamma}=\sigma_{\alpha\gamma}$.

The transition from a complete wetting (or nonwetting) regime to a partial wetting regime, or vice versa, is called a wetting transition. This remarkable interfacial phenomenon is the subject of intense current research[3,4] due to its importance in many industrial applications.

The wetting behavior of the middle C_iE_j-rich phase at the oil-water interface in ternary water+oil+C_iE_j mixtures had been extensively and systematically studied.[5–18] The symbol C_iE_j is the abbreviation of a nonionic polyoxyethylene alcohol $C_iH_{2i+1}(OCH_2CH_2)_jOH$. It was found that these ternary systems can exhibit diverse wetting behaviors by simply varying thermodynamic variables, such as temperature,[5–12] oil chain length,[13,15] amphiphilicity of an amphiphile,[6–10] and salinity.[17,18]

The most intriguing phenomenon observed in the water +n-alkane (such as octane, decane, dodecane, or tetradecane) +C_6E_2 system[12,13] was that the middle C_6E_2-rich phase would undergo a sequential wetting transition, nonwetting →partial wetting→complete wetting, along with increasing temperature. This observation verifies the suggestion that the wetting behavior can be related to the temperature dependence of the amphiphilicity of a surfactant.[6] These results are consistent with the critical-point wetting theory of Cahn[19] and of Ebner and Saam.[20]

Although the binary water+C_iE_j mixtures are relatively simpler than the ternary water+oil+C_iE_j mixtures, these systems also exhibit the intriguing phenomena in wetting behavior. The wetting behavior of the water+C_8E_j mixtures at 298.15 K was carefully investigated by Kahlweit and Busse.[6] These authors found that the contact angle θ of the suspended lens of the C_8E_j-rich phase at the air-water interface increases with an increase in the number of oxyethylene groups j from 0 to 3 stepwise. Based on this phenomenologi-

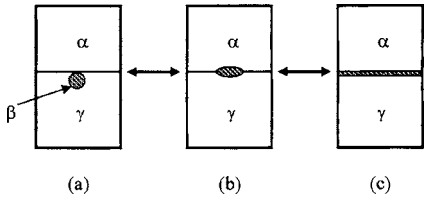

FIG. 1. Wetting behavior at a fluid-fluid interface. (a) A nonwetting β phase at α-γ interface, (b) a partial wetting β phase at α-γ interface, and (c) a complete wetting β phase at α-γ interface. The expected condition for only a small amount of the β phase at the α-γ interface.

[a)]Author to whom correspondence should be addressed. Electronic mail: ljchen@ntu.edu.tw

cal argument, Kahlweit and Busse[6] conjectured that it is possible to observe a wetting transition between nonwetting and partial wetting by the C_iE_j-rich phase at the air-water interface near the lower critical solution temperature (LCST) and another wetting transition between partial wetting and complete wetting near the upper critical solution temperature (UCST) in binary C_iE_j+water mixtures. In other words, the C_iE_j-rich phase in the water+C_8E_j mixtures exhibits a sequence of wetting transitions from nonwetting to partial wetting to complete wetting at the air-water interface along with increasing temperature from its LCST to UCST. To the best of our knowledge, this conjecture has not been experimentally verified.

The effect of the molecular structure of C_iE_j on the wetting behavior in the water+C_iE_j mixtures was carefully examined in our previous works,[21,22] which was still subject to relatively low temperatures. In this study, we assembled a new pendant bubble/drop tensiometer to extend our experimental temperature window up to 140 °C. Based on the experimental wetting coefficients, the wetting behavior in the binary water+C_4E_1 system was carefully investigated over the whole temperature range of its closed-loop miscibility gap (between temperatures 323.15 and 401.15 K).[23–25] This paper is organized as follows: The experimental details are described in the Sec. II. The results of the temperature dependence of the surface/interfacial tensions for the binary water+C_4E_1 system are presented. The wetting behavior of the C_4E_1-rich phase at the water surface is carefully discussed. Indeed, the occurrence of a sequence of wetting transitions in the binary water+C_4E_1 system is experimentally verified. Additionally, the interfacial tension between the C_4E_1-rich and aqueous liquid phases were verified to be strongly related to the miscibility gap.

II. EXPERIMENTS

A. Materials

Ethylene glycol monobutyl ether (n-C_4E_1, $>99\%$) was purchased from Merck Chemical Co., and used as received. Water was purified by double distillation and then followed by a PURELAB Maxima Series (ELGA LabWater) purification system with the resistivity always better than 18.2 MΩ cm.

B. Apparatus

A homemade pendant bubble/drop tensiometer was used to measure the interfacial tension between two coexisting liquid phases and the surface tensions of both liquid phases against helium. The schematic setup of the tensiometer is shown in Fig. 2. This device was mainly composed of a parallel light generator including a light source (model 190, fiber-optical illuminator, Dolan-Jenner), a diffuser, a pinhole, an achromatic lens, a solid-state monochrome change-coupled device (CCD) camera (XC-ST70, Sony), and a computer equipped with an image frame grabber (DT3155 MACH Series, Data Translation). The bubble (or liquid drop) image on the active area of the camera was magnified approximately 1× (or 1.8×) for surface- (or interfacial) tension measurement. The frame grabber digitized an image

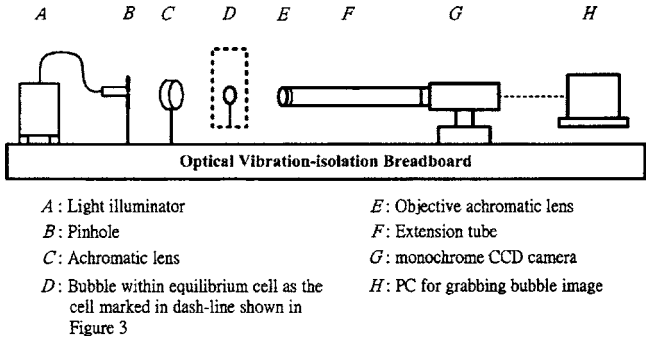

FIG. 2. The schematic setup of the pendant bubble/drop tensiometry.

into 640×480 pixels with an 8-bit resolution of 256 gray levels. The bubble (or liquid drop) forming system was composed of a precision syringe pump (model 100DM, ISCO Inc.) and stainless-steel needles. Two needles (Hamilton Co.) of different diameters, gauge 17 [1.07-mm inner diameter (i.d.); 1.47-mm outer diameter (o.d.)] and gauge 27 (0.21 -mm i.d.; 0.41-mm o.d.), were equipped at the bottom of the equilibrium cell for, respectively, the surface-and interfacial tension measurement. The glass liquid level gage (series 20) of JERGUSON Gage & Valve Co. was applied as the equilibrium cell. The sample mixture was held in the equilibrium cell, which was housed in a thermostat (TV4000, Tamson Labovisco, Holland). The temperature stability of the thermostat was better than ±0.05 K. The density for each phase was measured by using a vibrating-tube densiometer (DAM 60/512, Anton Paar, Austria) directly connected to the equilibrium cell through the pipeline and the liquid pump (LDC analytical minipump). We were able to measure the density online. The detailed layout of the experimental apparatus and the piping is schematically illustrated in Fig. 3.

C. Procedures

The equilibrium cell and all the pipelines were vacuumed by a vacuum pump (GCD-050XA, Sinku Kiko Co.,

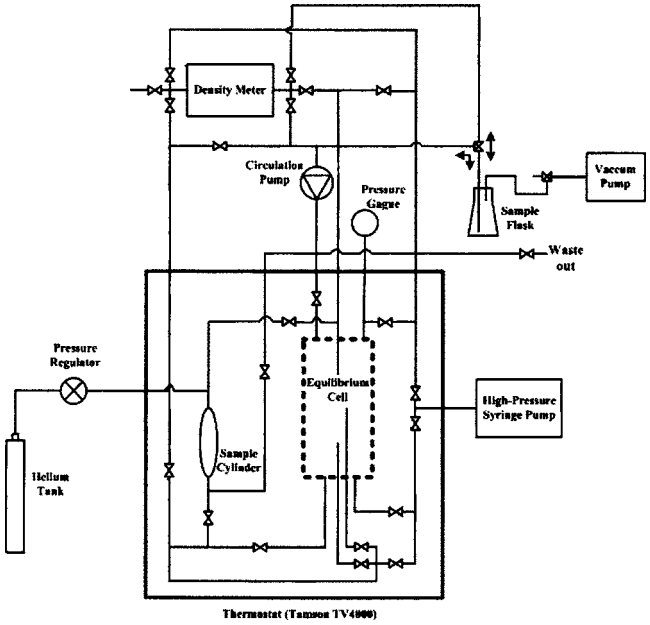

FIG. 3. The schematic setup of the experimental apparatus and the bubble/drop forming system.

Ltd. Japan). About 100 ml of degassed sample mixture with a proper composition (~0.3 mass fraction of $n-C_4E_1$) was automatically sucked into the equilibrium cell through the pipelines by pressure difference. The inert gas helium of 99.99% purity was then injected into the system to maintain the system at 10 bar, as indicated by a digital pressure gauge (DPI280/PDCR330, Druck Limited). The liquid sample in the equilibrium cell was circulated by the liquid pump for at least 2 h to ensure thorough mixing. The equilibration was established for at least several hours up to 1 day. When the equilibrium was reached, both the liquid phases in the equilibrium cell were clear and transparent with sharp and mirrorlike interfaces.

Note that a stainless-steel sample cylinder was assembled right beside the equilibrium cell, as shown in Fig. 3, for adjusting the level of the interface separating the C_4E_1-rich and aqueous phases in the equilibrium cell to perform the pendant bubble/drop method. The Hamilton needle for the pendant bubble/drop measurement was installed at the bottom of the equilibrium cell. Once the sample mixture was input, the whole needle was immersed in the lower aqueous phase after the equilibration. First we performed the surface-tension measurement for the lower aqueous phase. Then we had to pump a certain amount of the lower aqueous phase from the equilibrium cell to the sample cylinder to lower the level of the interface separating the C_4E_1-rich and aqueous phases, i.e., to ensure the tip of the needle right in the middle of the upper C_4E_1-rich phase for further surface-tension measurement for the upper C_4E_1-rich phase.

The precision syringe pump (model 100DM, ISCO Inc.) was applied to drive the upper fluid phase through the pipelines to form a bubble (or liquid drop) at the selected needle in the lower liquid phase. For each tension, at least ten different bubbles (or liquid drops) were formed. For each bubble (or liquid drop), at least ten images were taken for image analysis. An edge detection program was adopted from that of the previous work[26–28] to determine the bubble/drop profile from a digitized image. Once a bubble (or a liquid drop) profile was digitized and allocated, the selected-plane method was applied to determine the surface (or interfacial) tension by numerically fitting the profile to the Young-Laplace equation.[26–28] The experimental uncertainty of the surface-interfacial tension measurements was always better than 0.3%.

III. RESULTS AND DISCUSSION

It is well understood that the water+C_4E_1 system exhibits a closed-loop miscibility gap. Figure 4 shows the closed-loop phase diagram of the system.[23,24] Its LCST and UCST are, respectively, 49 and 129 °C.[23,24] We started with the system to perform its surface/interfacial tensions over its temperature window of closed loop at atmospheric pressure. However, when the temperature was higher than 85 °C, the mixture started boiling and no stable air-liquid interface was observed any more. Therefore, the inert helium was applied to increase the system pressure up to 10 bar, that suppressed thermal instability to gain stable interfaces for surface-interfacial tension measurements. Note that the closed-loop

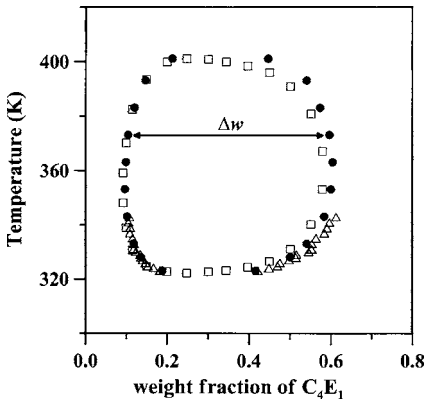

FIG. 4. Mutual solubility for the water+C_4E_1 binary system. Cox and Cretcher (Ref. 23) (□); Kim and Lim (Ref. 25) (△); Christensen *et al.* (Ref. 24) (●).

phase behavior of the water+C_4E_1 system would shrink as the system pressure increases.[29] However, 10 bar is still relatively a small pressure and too small to influence substantially the phase behavior of the mixture. The α, β, and γ phases defined in Fig. 1 correspond to the insert helium, C_4E_1-rich phase, and aqueous phase, respectively, in this liquid-liquid equilibrium system.

The surface/interfacial tensions for the water+C_4E_1 mixture at 10 bar were measured by the homemade pendant drop/bubble tensiometer between the upper and lower critical solution temperatures of the system. The experimental results of the surface tensions of the C_4E_1-rich phase ($\sigma_{\alpha\beta}$) and of the aqueous phase ($\sigma_{\alpha\gamma}$) are given in Figs. 5 and 6, respectively. Both surface tensions decrease along with increasing temperature. It should be noted that the experimental uncertainties for each data point are also given in Figs. 5 and 6. The error bars are always smaller than the size of open symbols.

Figure 7 shows the variation of experimental results of the interfacial tension between the C_4E_1-rich phase and the aqueous phase ($\sigma_{\beta\gamma}$) as a function of temperature ranging from its lower to upper critical solution temperature. The interfacial tension must be zero either at the lower or at the upper critical solution temperature of the system. To start with the lower critical solution temperature, the interfacial

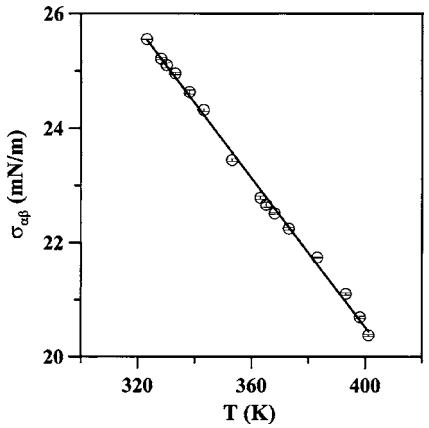

FIG. 5. Variation of surface tension $\sigma_{\alpha\beta}$ of the C_4E_1-rich phase as a function of temperature for the water+C_4E_1 system at 10 bar.

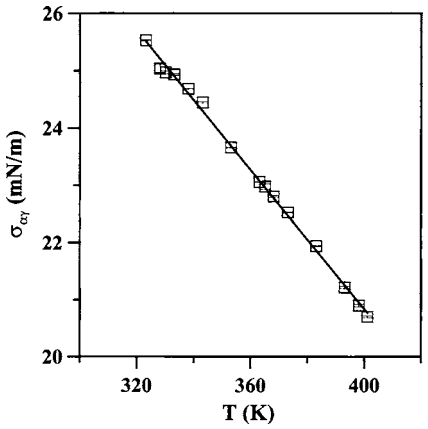

FIG. 6. Variation of surface tension $\sigma_{\alpha\gamma}$ of the aqueous phase as a function of temperature for the water+C_4E_1 system at 10 bar.

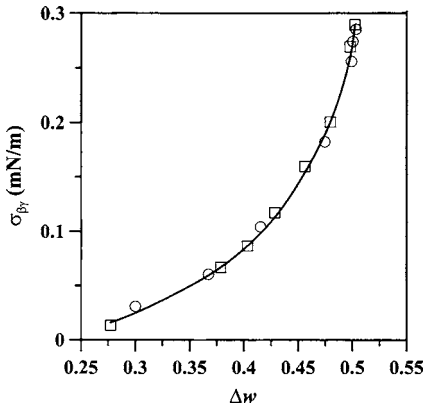

FIG. 8. Variation of the interfacial tension $\sigma_{\beta\gamma}$ as a function of the miscibility difference Δw. Experimental data below 90 °C (□) and above 90 °C (○).

tension $\sigma_{\beta\gamma}$ increases along with increasing temperature, reaches to a maximum around 90 °C, and then decreases along with increasing temperature. There is a qualitative rule for the interfacial tension related to the mutual solubility.[30] That is, the smaller the mutual solubilities, the greater the interfacial tension. Donahue and Bartell[31] proposed a linear relation between the interfacial tension of water-organic liquid interfaces and the logarithm of the "degree of miscibility," defined by $\ln(N_1+N_2)$, where N_1 is the mole fraction of the water in the organic liquid phase and N_2 is the mole fraction of the organic liquid in the aqueous phase. These authors had applied more than 30 organic liquids to verify that the interfacial tension decreases when $\ln(N_1+N_2)$ linearly increases *at constant temperature*.[31]

Instead of the "degree of miscibility," the miscibility difference Δw is proposed and defined by the difference between the weight fraction of C_4E_1 in the aqueous phase and that in the C_4E_1-rich phase, as schematically illustrated in Fig. 4. It is obvious that a large miscibility difference stands for a small mutual solubility. The variation of the miscibility difference Δw as a function of the temperature is also shown in Fig. 7 along with the interfacial tension. The miscibility difference Δw must be zero either at the lower or at the upper critical solution temperature of the system. To start with the lower critical solution temperature, the miscibility difference Δw increases along with increasing temperature, reaches to a maximum around 90 °C, and then decreases along with further increasing temperature, as shown in Fig. 7. As expected, the greater the miscibility difference Δw, the greater the interfacial tension. It is much more interesting to observe the variation of the interfacial tension as a function of the miscibility difference Δw, shown in Fig. 8, in which the square symbol stands for the data points of temperature below 90 °C and the circle symbol for that above 90 °C. Our experimental temperature range is from 50 to 128 °C. Both branches (below and above 90 °C) coincide with each other perfectly to form one curve. That implies the interfacial tension is strongly related to the miscibility difference Δw, and this relationship is *irrelevant to the temperature*, as illustrated in Fig. 8. It should be pointed out that Donahue and Bartell[31] found out that the interfacial tension linearly decreases along with an increase in $\ln(N_1+N_2)$ for more than 30 binary water+organic liquid mixtures only *at constant temperature*. However, our experimental data of interfacial tensions do not follow the linear dependence of $\ln(N_1+N_2)$.

The wetting behavior of the C_4E_1-rich phase at the interface separating the inert helium and the aqueous phase could be simply verified by the wetting coefficient. The wetting coefficients for the water+C_4E_1 system were determined from the surface/interfacial tensions. Figure 9 illustrates the variation of the wetting coefficient as a function of tempera-

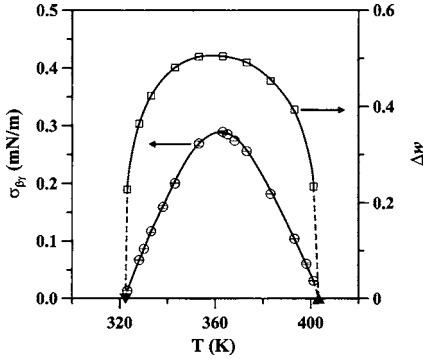

FIG. 7. Variation of interfacial tension $\sigma_{\beta\gamma}$ and the miscibility difference Δw as a function of temperature for the water+C_4E_1 system. $\sigma_{\beta\gamma}$ (○); Δw (□) [Christensen *et al.* (Ref. 24)], LCST (▼), and UCST (▲).

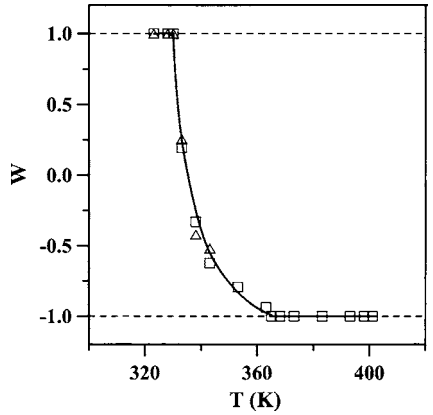

FIG. 9. Variation of wetting coefficient as a function of temperature for the water+C_4E_1 system at the normal pressure (△) and at 10 bar (□).

ture at 10 bar. In addition, the wetting coefficients determined at normal pressure are also shown in Fig. 9 by using the triangle symbol. These data (at normal pressure) coincide with that at 10 bar, as shown in Fig. 9. The pressure difference is too small to see the difference in wetting behavior, as expected.

The wetting behavior of the C_4E_1-rich (β) phase at the interface separating the helium and the aqueous phases for the water+C_4E_1 system is then classified into three regimes according to the wetting coefficient. They are (1) the nonwetting β phase with temperatures below 58.5 °C and with $W=1$, (2) the partial wetting β phase with temperatures in between 58.5 and 91 °C and with $1>W>-1$, and (3) the complete wetting β phase with temperatures above 91 °C and with $W=-1$.

To start with the system at 80 °C, the C_4E_1-rich phase exhibits partial wetting behavior at the surface of the aqueous phase. A wetting transition from partial wetting to nonwetting occurs at 58.5 °C while the system is brought to approach the LCST. This finding is consistent with that of Hirtz *et al.*[32] On the other direction, while the system is driven to approach the UCST, another wetting transition from partial wetting to complete wetting happens at 91 °C. In other words, a sequence of wetting transition, nonwetting → partial wetting → complete wetting, is observed in the water+C_4E_1 system with increasing temperature under 10 bar. Our results experimentally verify the conjecture of Kahlweit and Busse:[6] the existence of a wetting transition from nonwetting to partial wetting near the LCST and another wetting transition from partial wetting to complete wetting near the UCST for the binary mixture water +C_iE_j.

Figure 8 illustrates obviously that the wetting coefficient drops substantially right after the occurrence of the transition from nonwetting to partial wetting, then slowly decreases and "asymptotically" approaches −1 to trigger another transition from partial wetting to complete wetting by simply increasing the temperature. The order of the wetting transition between partial wetting and complete wetting is hard to identify based on our experimental accuracy. Currently we are in the process of using an ellipsometry to identify the order of this transition. On the other hand, the wetting transition between partial wetting and nonwetting is a first-order transition, consistent with previous experimental results [33,34] as well as with the theoretical prediction.[35,36] Currently, we are also in the process of using an ellipsometry to further verify this finding. Note that a hysteresis of the thickness of a wetting layer was found in the cyclohexane+methanol system,[34] consistent with the assumption of a first-order transition.

Previous experimental results[16,21,32] also demonstrated that for the binary mixtures water+C_6E_2 and water+$C_{10}E_4$ the wetting transition from nonwetting to partial wetting occurs near the LCST. However, these two systems are expected to have very high UCSTs, beyond the limitation of our apparatus. Therefore, we have no intention to perform the surface-interfacial tension measurements to further verify the existence of another wetting transition from partial wetting to complete wetting near its UCST. However, the inert gas phase can be replaced by an oil phase, then the binary water+C_iE_j system switches to the ternary water+oil+C_iE_j system. It is expected that the wetting behavior of the C_iE_j-rich phase at the oil-water interface in the ternary system would be similar to that of the C_iE_j-rich phase at the gas-water interface in the binary system, simply because both the inert gas and the oil are hydrophobic. More precisely, the inert gas is more hydrophobic than the oil. Thus, introduction of an alkane to the binary system would reduce the temperature difference between UCST and LCST,[15] that enables us to observe the wetting behavior over the whole temperature range in between UCST and LCST. For example, the UCST and LCST for the water+tetradecane +C_6E_2 system are 46.23 and 9.86 °C, respectively.[12] Indeed, the middle C_6E_2-rich phase in the water+tetradecane+C_6E_2 system would undergo a sequential wetting transition, nonwetting → partial wetting → complete wetting, at the oil-water interface along with increasing temperature.[12]

In this study, we already verified that the C_4E_1-rich phase in the water+C_4E_1 system would exhibit a sequence of wetting transitions, nonwetting → partial wetting → complete wetting, at air-water interface along with increasing temperature. Therefore, it is plausible to conjecture the existence of a sequential wetting transition, nonwetting → partial wetting → complete wetting, of the C_4E_1-rich phase at the oil-water interface in the ternary water+oil +C_4E_1 system. In previous studies, no such sequential wetting transition was observed. Chen *et al.*[11] as well as Kahlweit and co-workers[6–10] found that the C_4E_1-rich phase always completely wets the oil-water interface in the water +octane+C_4E_1 system over the whole temperature range in between UCST and LCST. On the other hand, another sequential wetting transition, complete wetting → partial wetting → complete wetting, of the C_4E_1-rich phase at the oil-water interface was observed in the water +octane+C_4E_1 system by Bonkhoff *et al.*[5] All these previous studies[5–11] are not consistent with the conjecture mentioned above. Thus, the wetting behavior of the C_4E_1-rich phase at the oil-water interface in the water+octane+C_4E_1 system remains a controversial problem. Currently, we are in the process of carrying out the surface-interfacial tension measurements to further verify the existence of a sequential wetting transition in the water+octane+C_4E_1 system.

IV. CONCLUSION

In this study, the surface-interfacial tension measurements were performed over the whole temperature range between UCST and LCST of the water+C_4E_1 system at 10 bar. Based on the wetting coefficient data, it is found that the C_4E_1-rich phase exhibits a sequence of wetting transitions, nonwetting → partial wetting → complete wetting, at the air-water interface by increasing the system temperature, consistent with the conjecture of Kahlweit and Busse.[6]

The interfacial tension is strongly related to the miscibility difference Δw over the whole temperature range of liquid-liquid equilibrium of the binary water+C_4E_1 system, as illustrated in Fig. 8. Note that this relationship is irrelevant to temperature.

ACKNOWLEDGMENTS

This work was supported by the National Science Council of Taiwan, Republic of China. We thank Professor Ming-Jer Lee for the help in assembling the apparatus.

[1] G. N. Antonow, J. Chim. Phys. Phys.-Chim. Biol. **5**, 372 (1907).
[2] F. P. Buff, in *Encyclopedia of Physics*, edited by S. Flugge (Springer, Berlin, 1960), Vol. 10, Sec. 7, pp. 298 and 299.
[3] G. Gompper and M. Schick, in *Phase Transitions and Critical Phenomena*, edited by C. Domb and J. L. Lebowitz (Academic, New York, 1994), Vol. 16.
[4] D. Bonn and D. Ross, Rep. Prog. Phys. **64**, 1085 (2001).
[5] K. Bonkhoff, A. Hirtz, and G. H. Findenegg, Physica A **172**, 174 (1991).
[6] M. Kahlweit and G. Busse, J. Chem. Phys. **15**, 1339 (1989).
[7] M. Aratono and M. Kahlweit, J. Chem. Phys. **95**, 8578 (1991).
[8] M. Kahlweit, R. Strey, M. Aratono, G. Busse, J. Jen, and K. V. Schubert, J. Chem. Phys. **95**, 2842 (1991).
[9] M. Kahlweit, R. Strey, and G. Busse, Phys. Rev. E **47**, 4197 (1993).
[10] M. Kahlweit and G. Busse, J. Phys. Chem. B **104**, 4939 (2000).
[11] L.-J. Chen, J.-F. Jeng, M. Robert, and K. P. Shukla, Phys. Rev. A **42**, 4716 (1990).
[12] L.-J. Chen and W.-J. Yan, J. Chem. Phys. **98**, 4830 (1993).
[13] L.-J. Chen, W.-J. Yan, M.-C. Hsu, and D.-L. Tyan, J. Phys. Chem. **98**, 1910 (1994).
[14] L.-J. Chen, S.-Y. Lin, and J.-W. Xyu, J. Chem. Phys. **104**, 225 (1996).
[15] L.-J. Chen, C.-D. Chiu, F.-S. Shau, W.-J. Cheng, and J.-G. Wu, J. Phys. Chem. B **106**, 12782 (2002).
[16] M.-C. Yeh and L.-J. Chen, J. Chem. Phys. **115**, 8575 (2001).
[17] L.-J. Chen and M.-C. Hsu, J. Chem. Phys. **97**, 690 (1992).
[18] L.-J. Chen, M.-C. Hsu, S.-T. Lin, and S.-Y. Yang, J. Phys. Chem. **99**, 4687 (1995).
[19] J. W. Cahn, J. Chem. Phys. **66**, 3667 (1977).
[20] C. Ebner and W. F. Saam, Phys. Rev. Lett. **38**, 1486 (1977).
[21] M.-C. Yeh, P.-C. Lin, and L.-J. Chen, J. Phys. Chem. B **108**, 9955 (2004).
[22] C.-K. Wu and L.-J. Chen, Langmuir **21**, 6883 (2005).
[23] H. L. Cox and L. H. Cretcher, J. Am. Chem. Soc. **48**, 451 (1926).
[24] S. P. Christensen, F. A. Donate, T. C. Frank, R. J. LaTulip, and L. C. Wilson, J. Chem. Eng. Data **50**, 869 (2005).
[25] K. Y. Kim and K.-H. Lim, J. Chem. Eng. Data **46**, 967 (2001).
[26] M.-C. Yeh, L.-J. Chen, S.-Y. Lin, and C.-T. Hsu, J. Chin. Inst. Chem. Eng. **32**, 109 (2001).
[27] S.-Y. Lin, L.-J. Chen, J.-W. Xyu, and W.-J. Wang, Langmuir **11**, 4159 (1995).
[28] S.-Y. Lin, L.-J. Chen, W.-J. Wang, and L.-W. Lin, Colloids Surf., A **114**, 31 (1996).
[29] M. Kahlweit and R. Strey, Angew. Chem., Int. Ed. Engl. **24**, 654 (1985).
[30] J. J. Bikerman, *Physical Surfaces* (Academic, New York, 1970), p. 118.
[31] D. J. Donahue and F. E. Bartell, J. Phys. Chem. **56**, 480 (1952).
[32] A. Hirtz, K. Bonkhoff, and G. H. Findenegg, Adv. Colloid Interface Sci. **44**, 241 (1993).
[33] J. W. Schmidt and M. R. Moldover, J. Chem. Phys. **79**, 379 (1983).
[34] D. Bonn, H. Hellay, and G. H. Wegdam, Phys. Rev. Lett. **69**, 1975 (1992).
[35] M.-C. Yeh and L.-J. Chen, J. Chem. Phys. **118**, 8331 (2003).
[36] M.-C. Yeh, C.-M. Chen, and L.-J. Chen, J. Phys. Chem. B **108**, 7271 (2004).